Investigation of the effect of fluid slip on heat transfer in the thin-film region in a micro-channel

Rama Subba Reddy Gorla and Dhruv V. Sharma
Department of Mechanical Engineering, Cleveland State University
Cleveland, Ohio 44115 USA

Abstract

A theoretical study was undertaken to check the influence of interfacial slip on evaporation of a thin liquid film in a microfluidic channel. The disjoining pressure and the capillary force which drive the liquid flow at the liquid-vapor interface in thin film region are adopted. The evaporating thin film region is an extended meniscus beyond the apparent contact line at a liquid/solid interface. Thin film evaporation plays a key role in a highly efficient heat pipe. Slip length was found to affect the heat transfer in the microchannel by altering the thin film geometry.

NOMENCLATURE

$\bar{A}$ dispersion constant (J)
h_{fg} latent heat of vaporization (J/kg)
k   thermal conductivity (W/m K)
K   curvature (1/m)
L   length of the thin film region (m)
$\bar{M}$ molecular weight (kg/mol)
m'' evaporative mass flux ($kg/m^2 s$)
P   pressure (Pa)
q'' heat flux (W/m^2)
$\bar{R}$ universal gas constant (J/mol K)
u velocity component in the x-direction (m/s)
x   x-coordinate (m)
y   y-coordinate (m)

Greek symbols

ρ density (kg/m^3)
β slip length (m)
δ film thickness (m)
v kinetic viscosity (m^2/s)
μ viscosity (N s/m^2)
σ surface tension (N/m)

Subscripts

0   presence of adsorbed region
c   capillary
d   disjoining
f   fluid
g   gas
l   liquid
s   solid
v   vapor
w   wall

1. INTRODUCTION

Technologies for heat dissipation have played an important role in the field of research on reliability, compactness and high performance of the electronic devices. These factors are the limelight of the latest technology that is advancing at a much faster rate by rigorous efforts put on by the researchers. Enhancement of heat transfer by the phase change technique has been heeded in chemical processing equipment and nuclear reactor and also in electronic cooling. Capillary pumped loop systems that fall under the category of capillary heat pumps have been used successfully for this application. Increase in density and miniaturization of the electronics component has been achieved by the advancement of packaging technology. Hence it becomes of prime importance to get rid of the excess heat generated in the micro-scale devices that are supposed to work at a relatively lower temperature. The micro-CPL system consists of the evaporator, condenser, vapor and liquid lines and can be applicable to the small-scale device that uses phase change to transfer thermal energy and it belongs to the application of MEMS (micro-electro-mechanical systems). Extended meniscus is divided into three parts as shown in Figure 1, when a liquid comes into contact with a solid surface; (1) the intrinsic meniscus region which is overpowered by the capillary forces, (2) the evaporating thin film region which is controlled by the concocted effects of both capillary and disjoining pressure, and (3) the adsorbed region where the evaporation does not occur. Out of the aforesaid points, most important region is the thin-film region where abundant heat is transferred.
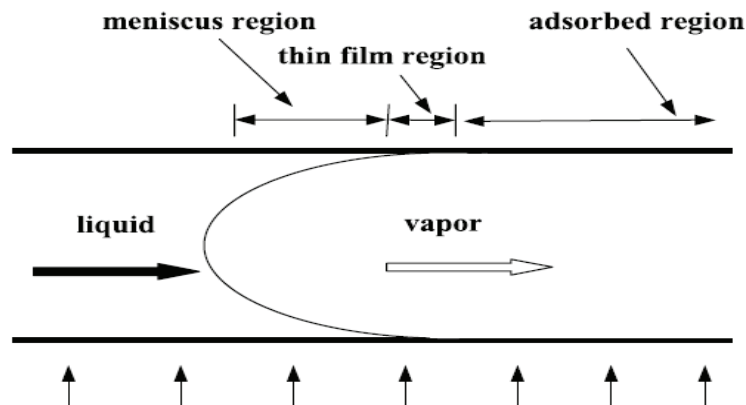

Figure 1. Three regions showing the liquid evaporation system in a microchannel.

The thin film evaporating region consists of an extended meniscus beyond the apparent contact line at a liquid/solid interface, which is formed as a combined consequence of the capillary and disjoining pressure effects in the interfacial region. Several efforts have been wielded for the performance of the extended meniscus on a flat plate by establishing the analytical models and conducting experiments for the last several years. Since Derjaguin [1] first analyzed the thermo-fluid characteristics of an evaporating thin film region, a number of excellent numerical and experimental investigations [2-4] have been introduced to predict the flow and heat transfer for various evaporator specifications. Das Gupta et. al. [5] studied the transport processes occurring in an evaporating extended meniscus. They suggested the augmented Young-Laplace equation with Kelvin-Clapeyron equation and kinetic theory that can be used to model fluid flow and evaporative heat transfer in the contact line region. Longtin et. al. [6] proposed a mathematical model to predict the heat transfer in a micro heat pipe having a triangular cross section. They concluded that the radius of curvature increases linearly along the flow direction. Sartre et. al. [7] presented a three dimensional model for predicting heat transfer in an extended meniscus region of a micro heat pipe array. They reported that the apparent contact angle and

the heat transfer rate increase with increasing wall superheat. Qu et. al. [8] proposed a model to account for the formation of evaporating thin film and meniscus in capillary tubes. They investigated the effects of radius and heat transfer on the profile if evaporating extended meniscus region. Relation between the rate of evaporation from thin film liquid at a saturation temperature and its respective pressure with the vapor phase mass diffusion was established by Biswal et al. [9]. A detailed model to determine the effects of inertial force, interfacial thermal resistance, surface tension, and disjoining pressure on the thin film profile, interfacial temperature variation, fluid flow, and the local heat transfer rates was developed by Ma et al. [10].

The afore-mentioned investigations on the analysis of thin film evaporation are based on the presumption that the classical pattern of no slip boundary condition, exists at the fluid-solid interface in the thin film region. Fundamentally, this belief may often be justified from the assumption that liquid elements may settle within the surface unevenness, leaving it impossible for the molecules to get away from the interfacial contacts due to the compact molecular packing arrangement. Nevertheless, this argument may contradict for systems with little less molecular densities over an interfacial layer that may be caused by numerous thermo-physical activities of which, one is hydrophobic interactions near surface roughness elements. The later may induce the formation of an ultra-thin depleted layer adhering to the channel walls, typically of tens of nanometers in dimensions that may act as a slip agent by prohibiting the liquid to come in contact with the surface elements. Since the depleted layer may not be visible from microscopic viewpoint, it is termed as apparent slip.
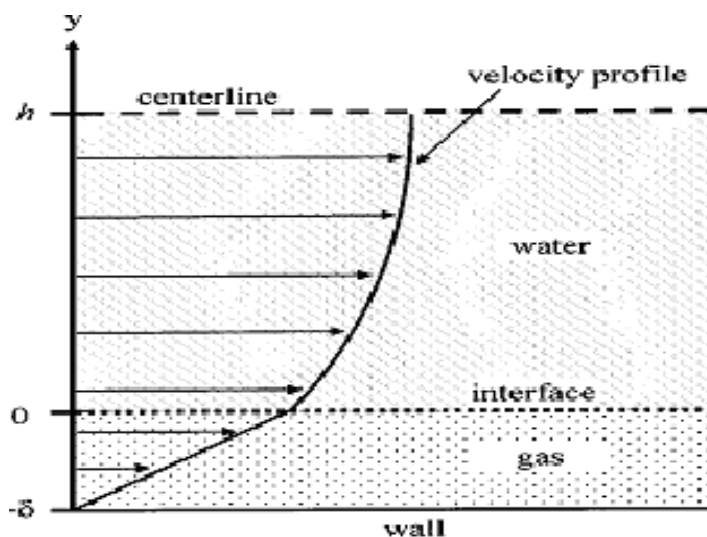

Figure 2. Physical model of fluid distribution between two infinite parallel plates proposed by Tretheway and Meinhart.

2. FLUID SLIP GENERATION
There are many significant differences between fluid flow at macro scale and that at micro/nano scale, e.g., wall-slip phenomena. Effects of slip conditions are very important for some fluids that exhibit wall slip. Fluids exhibiting slip are important in technological applications such as in the polishing of artificial heart valves, internal cavities and polymer melts. Therefore, a better understanding of the slip phenomena is necessary. With a hot-wire anemometer , Watanabe et al. [11-12] identified fluid slip at the wall of a strongly hydrophobic duct or pipe. Their velocity profiles are consistent with Navier's hypothesis [13]. Ruckenstein and Rajora [14] investigated fluid slip in glass capillaries with surfaces made repellent to the flowing liquid. Their experimental results of pressure drop indicate larger slip

than that predicted by chemical potential theory, where slip is proportional to the gradient in the chemical potential. Mooney [15] studied the boundary layer flows with partial slip. Many researchers [16–17] had confirmed the phenomena of wall-slip fluids.

Tretheway and Meinhart's [18] proposed model in Figure 2 calculates the bubble height or air gap required to generate measured slip lengths, assuming Navier's hypothesis effectively describes a thin air gap at the surface.
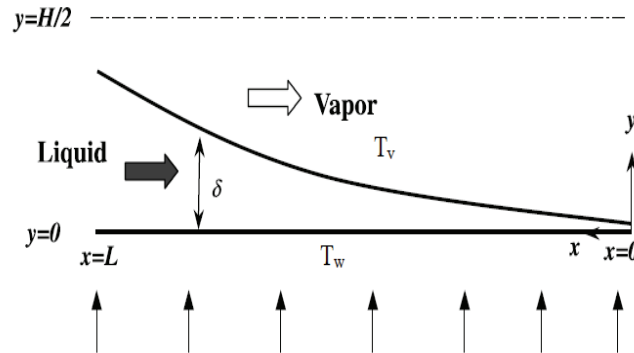

Figure 3. Coordinate system of the lower half of the microchannel

Navier's hypothesis states that the velocity at a surface is proportional to the shear rate at the surface

$$u(y = 0) = \beta(du / dy)_{y=0}$$

where β has units of length and is defined as the slip length.

Tretheway and Meinhart [18] developed an analytical model to quantify the effects of an air gap on fluid flow between two infinite parallel plates. Experimental observation by Tretheway and Meinhart [18] and Zhu and Granick [19] showed by calculating slip lengths that the presence of nanobubbles or a low viscosity layer may be responsible for the apparent fluid slip. The effects of nanobubbles and hydrophobicity could be mitigated by employing higher absolute pressures and smooth surfaces at atomic level were explained by Choi et al. [20] by measuring substantially smaller slip lengths. At last, the fluid slip generated from rarefied gas conditions turn out to be overestimated by the simplified two-dimensional analytical solutions. Hence, to understand the effects of hydrophobic surfaces that persist in microchannel fluid flow, elaborated numerical simulations are necessary.

3. MATHEMATICAL PROCEDURE

The geometrical configuration and the coordinate system for the evaporating thin film flow in a microchannel are shown in Figure 3. T_w is the wall temperature that is constant and greater than T_v vapor temperature, P_v is the vapor pressure and the meniscus is superheated. We consider only the lower half of the micro-channel because of the geometric symmetry.

The following assumptions are employed in the derivation of the governing equations:
- A steady-state two-dimensional laminar flow,
- Incompressibility of the liquid and   the vapor,
- Constant fluid properties and surface tension,

Using Young-Laplace equation to express the pressure difference between vapor and liquid at the liquid-vapor interface which is caused by capillary pressure P_c and disjoining pressures,

$$P_v - P_1 = P_c + P_d \tag{1}$$

Where Pd is the disjoining pressure and is expressed as,

$$P_d = -\overline{A}\big/\delta^3 \tag{2}$$

$\overline{A}$ is the dispersion constant and δ the film thickness.

Capillary pressure is defined as the product of interfacial curvature K and the surface tension coefficient σ.

$$P_c = \sigma K, \ K = \frac{\delta''}{\left(1+\delta'^2\right)^{1.5}} \tag{3}$$

Combining Eqs. (1), (2) and (3) and differentiating with respect to x, a third order differential equation is obtained for $\delta(x)$.

$$\frac{d^3\delta}{dx^3} - 3\left(\frac{d\delta}{dx}\right)\left(\frac{d^2\delta}{dx^2}\right)^2\left[1+\left(\frac{d\delta}{dx}\right)^2\right]^{-1} + \frac{1}{\sigma}\left(\frac{dP_l}{dx} - \frac{3\overline{A}}{\delta^4}\frac{d\delta}{dx}\right)\left[1+\left(\frac{d\delta}{dx}\right)^2\right]^{-1.5} = 0 \tag{4}$$

Rearranging Eq. (4) gives

$$\frac{dP_l}{dx} = -\frac{\sigma\delta'''}{\left(1+\delta'^2\right)^{1.5}} + \frac{3\sigma\delta'\delta''^2}{\left(1+\delta'^2\right)^{2.5}} - \frac{3\overline{A}}{\delta^4}\delta' \tag{5}$$

Employing, lubrication theory for the momentum equation for the liquid in the thin film region yields,

$$\mu_l \frac{\partial^2 u}{\partial y^2} = \frac{dP_l}{dx} \tag{6}$$

where μ_1 and P_1 are the liquid phase viscosity and pressure respectively.

Integration of Eq. 6, using the slip boundary condition $u_s = \beta\left(\partial u\big/\partial y\right)_w$ at y = 0 twice with a note that $\partial u\big/\partial y \approx 0$ at y = δ yields,

$$u = \frac{1}{2\mu_l}\frac{dP_l}{dx}\left(y^2 - 2\delta y - 2\beta\delta\right) \tag{7}$$

Estimation of net rate of evaporation by considering a mass balance over a differential section of the liquid film of axial length dx pertaining to Eq. (7) yields,

$$\frac{d\dot{m}_x}{dx} = -m'' \tag{8}$$

where m" is the evaporation mass flux and related to Eq. (7), $\dot{m}_x$ is the rate of mass transfer at any section x given as,

$$\dot{m}_x = \rho_l \int_0^\delta u \, dy \qquad (9)$$

Substituting Eq. (7) in Eq. (9), it gives,

$$\dot{m}_x = -\frac{\delta^3 + 3\beta\delta^2}{3v_l} \frac{dP_l}{dx} \qquad (10)$$

where v_l is the Kinematic viscosity of the liquid phase.
Combining Eqs. (8) and (10), it gives

$$\frac{dP_l}{dx} = \frac{3v_l}{\delta^3 + 3\beta\delta^2} \int_0^x m'' \, dx \qquad (11)$$

Now Substituting Eq. (4) in (11), it follows

$$\frac{d}{dx}\left[\left\{\frac{\sigma\delta'''}{(1+\delta'^2)^{1.5}} - \frac{3\sigma\delta'\delta''^2}{(1+\delta'^2)^{2.5}} + \frac{3\overline{A}}{\delta^4}\delta'\right\}\frac{(\delta^3 + 3\beta\delta^2)}{3v_l}\right] = -m'' \qquad (12)$$

Assuming the surface tension coefficient to be zero, the above equation reduces to

$$\frac{d}{dx}\left[\frac{(\delta^3 + 3\beta\delta^2)}{3v_l}\frac{3\overline{A}}{\delta^4}\delta'\right] = -m'' \qquad (13)$$

Dispersion Constant $\overline{A}$ is assumed to be - 2.87×10^{-21}J.
Now, the evaporation mass flux m" and the associated terms are adopted from Wang et al. [21],

$$m'' = \frac{1}{h_{fg}}\frac{h_{lv}k_l(T_w - T_v)}{k_l + h_{lv}\delta} \qquad (14)$$

h_{lv} is the evaporative heat transfer coefficient,

$$h_{lv} = ah_{fg}$$

where $a = C\left(\dfrac{\overline{M}}{2\pi\overline{R}T_{lv}}\right)^{1/2}\dfrac{P_v\overline{M}h_{fg}}{\overline{R}T_vT_{lv}}$, deduced from Wang et al. [21]. h_{fg} is the latent heat of evaporation

(J/kg). Water is used as the working fluid at a saturation temperature of approximately 383 K. The properties are shown in Table 1.

Table 1. Properties of H2O as the working fluid at 383K

Properties	Values	Properties	Values
Dispersion constant($\bar{A}$)	2.87×10^{-21} J	Viscosity of liquid (μ_l)	2.82×10^{-4}N/sm^2
Latent heat of evaporation (h_{fg})	2.256×10^6J/kg	T_w (K)	383
Thermal conductivity (k_l)	0.68 W/m K	T_v (K)	382
Density of liquid (ρ_l)	958.31 kg/m^3	C (accommodation coefficient)	2

For the film thickness, the governing equation Eq. (13) is a second-order non-linear ordinary differential equation. The right hand side of Eq. (13) is assumed to be constant for simplification purpose and then the method of separation for nonlinear differential equations is applied preceded by simple integration with respect to x. The boundary conditions for the film thickness at x = 0 are as follows:

$$\delta_{(x=0)} = \delta_0, \quad \left(\frac{d\delta}{dx}\right)_{(x=0)} = 0 \quad , \quad \left(\frac{d^2\delta}{dx^2}\right)_{(x=0)} = 0 \tag{15}$$

Ideally, δ_0 which is the film thickness at x = 0 is of the order of 10^{-9} m.

4. RESULTS

Figure 4 shows the variation of liquid film thickness (δ) along the length of the microchannel for the fluid slip ($\beta = 0$) between the film and the channel wall. It is observed that the film thickness decreases continuously in the direction of flow, as β increases. It presents a profile of the flow geometry similar as shown in Figure 3. Nevertheless, the almost parallel trend at the start in fig 4 is due to the adsorbed region that manifests constant film thickness. Figure 5 shows the effect of variation of slip values on the film thickness. It shows that as the slip length increases the length of the thin film region also
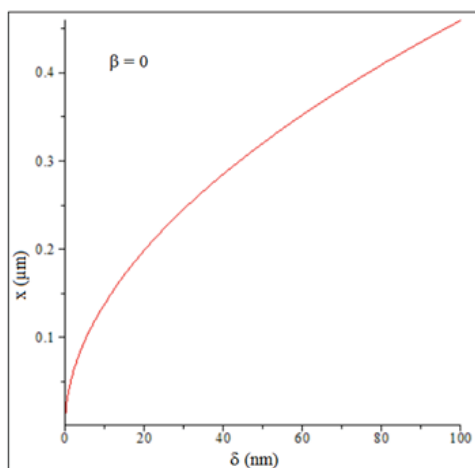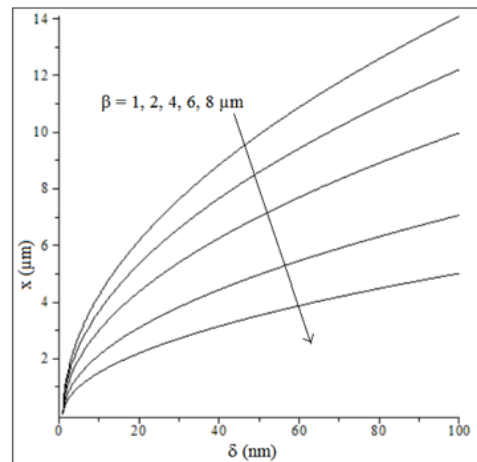
Figure 4. Variation of δ at no-slip condition

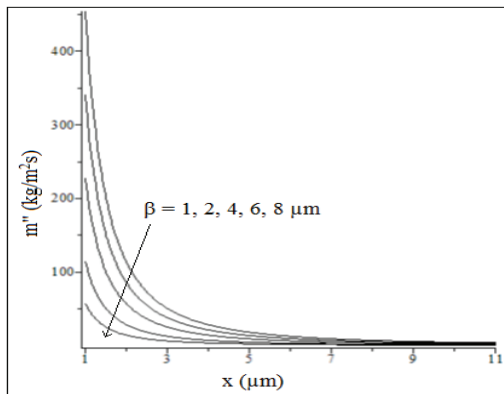Figure 5. Variation of δ at different slip values

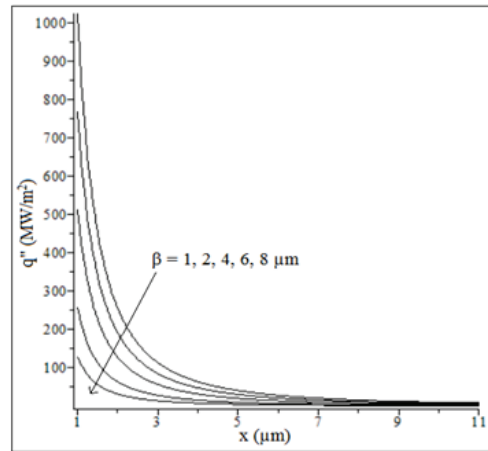Figure 6. Variation of mass flux at different slip length values

Figure 7. Variation of heat flux at different slip values

increases thereby decreasing the mass flux in the liquid-vapor interface region.

Evaporative mass flux as visible in Figure 6, is decreasing drastically moving from thin-film region and approaching to adsorbed region and then going almost parallel. Mass flux also depends on the temperature difference (T_w-T_v) and it increases with increase in temperature difference between the wall and vapor.   But here, it is assumed to be unity. The heat flux (q") is determined by the film thickness (?) and the temperature difference (T_w-T_v). The initial high value is due its transition in the thin film region and then the decreasing trend is due to the adsorbed region where the film thickness is almost constant and minimal. Temperature decrease in the adsorbed region also contributes to the decrease of heat flux along with the decrease in vapor pressure that causes the film likely to disappear. Evaporation rate near the adsorbed region decreases because of the high disjoining pressure and low temperature difference as the likely happens near the meniscus region due to high capillary pressure as presented in L Biswal et al. Figure 7 shows that heat flux decreases with the increase in slip length as it elongates the thin film and thereby making it more thicker and that in turn, decreases the heat flux and mass flux.

Table 2 shows a comparison of our results with those of Wang et al. [21]. These results show that our results are accurate.

Table 2. Thin film region results (Intrinsic meniscus radius = 250 nm) for β = 0

	Present results	results of Wang et al. [21]
Thin film length (nm)	155	154
Film thickness (nm)	21	21
Heat transfer rate (W/m)	0.139	0.139

5. CONCLUSION

An investigation was carried out to check the effect of apparent slip in the microchannels that indicates the presence of depleted gas layer near the wall surface.

It was found that the liquid film thickness follows a decreasing trend along the direction of flow and then exhibits a flat trend. This flat trend demonstrates a thin film of minimal thickness that represents the adsorbed region. Decreasing from the peak value to a minimum value and then a constant flat trend in heat flux and evaporative mass flux substantiates the transition from thin film region to the adsorbed region in the flow direction. As the value of slip length increases the subsequent peak values of the heat flux and mass flux decrease thereby proving that the slip length has a negative effect on the heat and mass transfer within the microchannel and it is necessary to find out the possible reasons for its formation so as to curb its growth.

REFERENCES

[1]   B.V. Derjaguin, and Z.M. Zorin, "Optical Study of the Absorption and Surface Condensation of Vapors in the Vicinity of Saturation on a Smooth Surface," *Proc.2nd International Congress on Surface Activity* (London), 2, (1957), 145-152.

[2]   X. Xu, and V.P. Carey, "Film Evaporation from a Microgrooved Surface: An Approximate Heat Transfer Model and its Comparison with Experimental Data," *AIAA Journal of Thermophysics*, 4, (1990), 512-520.

[3]   J.M. Ha, and G.P. Peterson, "The Interline Heat Transfer of Evaporating Thin Film Along a Micro Grooved Surface," *ASME Journal of Heat Transfer*, 118, (1996), 747-755.

[4]   K. Park, K.J. Noh, and K.S. Lee, "Transport Phenomena in the Thin Film Region of a Micro Channel," *International Journal of Heat and Mass Transfer*, 46, (2003), 2381-2388.

[5]   S. Das Gupta, I.Y. Kim, and P.C. Wayner, "Use of Kelvin-Clapeyron Equation to Model an Evaporating Curved Microfilm," *J. Heat Transfer, Trans. ASME*, 116, (1994), 1007-1015.

[6]   J.P. Longtin, B. Badran, and F.M. Gerner, "A One Dimensional Model of a Micro Heat Pipe During Steady State Operation," *ASME Journal of Heat Transfer*, 116, (1994), 709-715.

[7]   V. Sartre, M. Zaghdoudi, and M. Lallemand, "Effect of Interfacial Phenomena on Evaporative Heat Transfer in Micro Heat Pipes," *International Journal of Thermal Sciences,* 39, (2000), 498-504.

[8]   W. Qu, T. Ma, J. Miao, and J. Wang, "Effects of Radius and Heat Transfer on the Profile of Evaporating Thin Liquid Film and Meniscus in Capillary Tubes," *International Journal of Heat and Mass Transfer*, 45,(2002),1879-1887.

[9]   L. Biswal, S. K. Som and S. Chakraborty, "Thin film evaporation in microchannels with interfacial slip" Microfluid Nanofluid (2011) 10:155–163

[10]   H.B. Ma, G.P. Peterson, Temperature variation and heat transfer in triangular grooves with an evaporating film, J. Thermophys. Heat Transfer 11 (1997) 90–97.

[11]   2. K. Watanabe, Yanuar, and H. Mizunuma, Slip of Newtonian Fluids at Slid Boundary, JSME International Journal Series B**,** 41, 525-529 (1998).

[12]   3. K. Watanabe, Yanuar, and H. Udagawa, Drag Reduction of Newtonian Fluid in a Circular Pipe With a Highly Water-Repellant Wall, J. of Fluid Mechanics, 381, 225-238 (1999).

[13]   4. E. Ruckenstein, and P. Rajora, On the No -Slip Boundary Condition of Hydrodynamics, J. of Colloid and Interface Science, 96, 488-491 (1983).

[14]   5. M. Mooney, Explicit formulas for slip and fluidity. Journal of Rheology, 2(2), 210–222 (1931).

[15]   6. I. J. Rao, and K. R. Rajagopal, The effect of the slip condition on the flow of fluids in a channel, Acta Mech. ,135(3), 113–126 (1999).

[16]   7. A. R. A. Khaled, and K. Vafai, The effect of slip condition on Stokes and Couette flows due to an oscillating wall: exact solutions, Int. J. Non-Linear Mech, 39(5), 795–804 (2004).

[17]   Tretheway and Meinhart, "A generating mechanism for apparent fluid slip in hydrophobic microchannels" Physics of Fluids (2004) Vol 16: 5-14.

[18]   CLMH Navier. M´emoire sur les lois du mouvement des fluides. Mem. Acad. R. Sci. Paris.,6:389–416, 1823.

[19]   Y. Zhu and S. Granick, ''Limits of the hydrodynamic no-slip boundary condition'' Physics Reviewe Letters (2002) Vol 88: 10-17.

[20]   Choi CH, Johan K, Westin A, Breuer KS, "Apparent slip flows in hydrophilic and hydrophobic microchannels" Physics of Fluids (2003) 15:2897–2902

[21]   Wang H, Garimella SV, Murthy JY, "Characteristics of an evaporating thin film in a microchannel" International Journal of Heat Mass Transfer (2007) 50:3933–3942